Monthly Notices
of the
ROYAL ASTRONOMICAL SOCIETY

MNRAS **431,** 1678–1685 (2013)
Advance Access publication 2013 March 8

doi:10.1093/mnras/stt288

On the activity of the γ-Ursae Minorids meteoroid stream in 2010 and 2011

José M. Madiedo,[1,2]⋆ Josep M. Trigo-Rodríguez,[3] Esko Lyytinen,[4] Joan Dergham,[3] Pep Pujols,[5] José L. Ortiz[6] and Jesús Cabrera[2]

[1]*Facultad de Ciencias Experimentales, Universidad de Huelva, 21071 Huelva, Spain*
[2]*Departamento de Física Atómica, Facultad de Física, Universidad de Sevilla, Molecular y Nuclear, 41012 Sevilla, Spain*
[3]*Institut de Ciències de l'Espai (CSIC-IEEC), Campus UAB, Facultat de Ciències, Torre C5-parell-2ª, 08193 Bellaterra, Barcelona, Spain*
[4]*Kehäkukantie 3B, 00720 Helsinki, Finland*
[5]*Agrupació Astronómica d'Osona (AAO), Carrer Pare Xifré 3, 3er. 1a. 08500 Vic, Barcelona, Spain*
[6]*Instituto de Astrofísica de Andalucía, CSIC, Apt. 3004, Camino Bajo de Huetor 50, 18080 Granada, Spain*

Accepted 2013 February 13. Received 2013 February 8; in original form 2012 November 16

ABSTRACT

Accurate orbital data obtained for the recently discovered γ-Ursae Minorids meteoroid stream during the 2010 and 2011 Spanish Meteor Network and Finnish Fireball Network observing campaigns are presented. In particular, we focus on an outburst detected in 2010 and on the analysis of the first emission spectrum recorded for a member of this meteoroid stream. An array of high-sensitivity CCD video devices operating from different locations in Spain and Finland was used to perform this study. We have obtained precise trajectory, radiant and orbital information for seven members of this stream. Considerations about its likely parent body based on orbital dissimilarity criteria are made. We also present an estimation of the tensile strength for these meteoroids and a unique emission spectrum of a γ-Ursae Minorid fireball that reveals that the main rocky components have chondritic abundances.

Key words: meteorites, meteors, meteoroids.

1 INTRODUCTION

The recently discovered γ-Ursae Minorids (GUM) meteoroid stream was first detected by means of radar observations (Brown et al. 2010). It was then introduced in the IAU working list of meteor showers with the code 404 GUM. This stream exhibited an outburst of relatively bright meteors, with an average absolute magnitude of about 0.55, around 2010 January 20–21, and several single and multiple station trails were imaged by Finnish observers by means of wide-angle CCD video cameras (Jenniskens 2010). Here we present a significant progress in our knowledge of this meteoroid stream on the basis of continuous and exhaustive monitoring of the night sky using high-sensitivity CCD video devices.

Additional observations of the GUM stream can provide useful information in order to improve our knowledge about its origin, evolution and activity period. One of our goals is the determination of high-precision orbits, as these can provide important clues to establish, for instance, which is the likely parent body of this swarm. With this aim, the Finnish Fireball Network (FN) and the SPanish Meteor Network (SPMN) organized a joint campaign to monitor this stream during 2010 and 2011 January by means of high-sensitivity CCD video devices. These systems have the advantage that fainter meteors can be registered when compared to photographic or slow-scan all-sky CCD techniques, although the lower spatial resolution of these video devices implies that several cameras must be used to cover the whole sky.

Despite bad weather over Finland and Spain prevented a continuous monitoring of the shower display, 12 single and multi-station GUM meteor trails were recorded from January 10 to 22. For events simultaneously recorded from at least two stations, atmospheric trajectory, radiant and orbital information were derived. Thus, as a result of this joint effort, in this paper we provide additional data on this poorly known meteoroid stream. These include not only the above-mentioned orbital data, but also tensile strength measurements and information about the chemical composition of GUM meteoroids inferred from the analysis of the emission spectrum produced by a GUM fireball (absolute mag. -5.0 ± 0.5) recorded on 2011 January 20.

2 INSTRUMENTATION AND DATA REDUCTION TECHNIQUES

The observation of the GUM was made in 2010 and 2011 from several video meteor stations operated from Finland and Spain (Table 1). These are based on unintensified low-light monochrome

⋆E-mail: madiedo@cica.es

Table 1. Geographical coordinates of the meteor observing stations involved in this work.

Station no.	Station name	Longitude	Latitude (N)	Alt. (m)
1	Sevilla	05° 58′ 50″ W	37° 20′ 46″	28
2	La Hita	03° 11′ 00″ W	39° 34′ 06″	674
3	Huelva	06° 56′ 11″ W	37° 15′ 10″	25
4	Folgueroles	02° 19′ 33″ E	41° 56′ 31″	580
5	Montseny	02° 32′ 01″ E	41° 43′ 47″	194
6	Montsec (OAdM)	00° 43′ 46″ E	42° 03′ 05″	1570
7	Sierra Nevada	03° 23′ 05″ W	37° 03′ 51″	2896
8	El Arenosillo	06° 43′ 58″ W	37° 06′ 16″	40
9	Pieksämäki	27° 06′ 34″ E	62° 15′ 37″	145
10	Joutsa	26° 06′ 37″ E	61° 44′ 27″	135
11	Järvenpää	25° 07′ 39″ E	60° 29′ 39″	60
12	Kuusankoski	25° 35′ 33″ E	60° 54′ 14″	94

CCD video systems that our team employs since 2006 for the analysis of meteor activity (Madiedo & Trigo-Rodríguez 2007; Trigo-Rodríguez et al. 2007). In general, our video meteor stations employ between four and nine high-sensitivity Watec CCD video cameras (models 902H and 902H Ultimate from Watec Corporation, Japan) to monitor the night sky. These CCD video cameras generate interlaced video imagery at 25 fps with a resolution of 720×576 pixels (PAL video system). They are equipped with a 1/2 arcsec Sony interline transfer CCD image sensor with their minimum lux rating ranging from 0.01 to 0.0001 lux at *f*1.4. Aspherical fast lenses with focal lengths ranging from 4 to 6 mm and focal ratios between 1.2 and 0.8 are used for the imaging objective lens. In this way, different areas of the sky can be covered by every camera, and point-like star images are obtained across the entire field of view. Besides, this configuration allows us to record meteors of up to 3 ± 1 stellar magnitude. The cameras are connected to a computer via a video acquisition card. Different PCI and USB 2.0 video acquisition cards have also been tested and employed. In most cases, a better performance for internal PCI cards has been found. According to our experience, USB acquisition cards tend to fail or get damaged more often, although they are very useful mainly for mobile stations based on portable computers. The computers use the UFOCAPTURE software (Sonotaco, Japan) to automatically detect meteor trails and store the corresponding video sequences on hard disk. On the other hand, the cameras are arranged in such a way that the common atmospheric volume monitored by neighbouring stations is maximized. This was accomplished by using the program *Photographic centers for multiple station meteor observations* in the same way as was explained in Trigo-Rodríguez et al. (2004b). Besides, some of our observing stations work in an autonomous way by means of own software (Madiedo & Trigo-Rodríguez 2010; Madiedo et al. 2010) and have attached holographic diffraction gratings (500 or 1000 lines mm^{-1}, depending on the device) to record the emission spectra resulting from the ablation of meteoroids in the atmosphere. A more detailed description of these systems has been given elsewhere (Madiedo & Trigo-Rodríguez 2007, 2010).

The first step in the data reduction process implies the identification of meteor trails simultaneously recorded from, at least, two different observing stations. This is automatically done by means of one of our software packages, which performs a search through the data base of meteors that appeared during the same observing interval and in the proper position. Then, an astrometric measurement is done in order to obtain the plate (x, y) coordinates of the meteor along its apparent path from each station. The position of the meteor in each video frame is measured by hand. Special care is taken with those frames where the meteor trail spreads over a large number of pixels, as these can lead to higher errors. Thus, those positions that give rise to high deviations in the calculation of the deceleration curve are measured again or discarded. These meteor positions are introduced in our AMALTHEA software (Trigo-Rodríguez, Madiedo & Williams 2009; Madiedo, Trigo-Rodríguez & Lyytinen 2011a), which transforms plate coordinates into equatorial coordinates by using the position of reference stars appearing in the images. This package employs the method of the intersection of planes to determine the radiant and reconstruct the trajectory in the atmosphere of meteors recorded from at least two different observing stations (Ceplecha 1987). From the sequential measurements of the video frames and the trajectory length, the velocity of the meteor along its path is obtained. The pre-atmospheric velocity V_∞ is found by measuring the velocities at the earliest part of the meteor trajectory. Once this velocity and the atmospheric trajectory are known, the software computes the orbital parameters of the corresponding meteoroid by following the procedure described in Ceplecha (1987). Orbital parameters were found to be consistent with other previously tested software packages (Madiedo & Trigo-Rodríguez 2007, 2010).

3 OBSERVATIONS: TRAJECTORY, RADIANT AND ORBITAL DATA

In total, seven double-station GUM were recorded during our joint observing campaigns in 2010 and 2011. These events are listed in Table 2, where the SPMN and FN codes are used for identification. The analysis of these trails allows the determination of their atmospheric trajectory and the corresponding orbital parameters.

GUM meteors recorded during the 2010 outburst were relatively bright, with a mean magnitude of +0.55 and a magnitude distribution index of $\chi = 1.65 \pm 0.35$ (Jenniskens 2010). This magnitude distribution probably suggests a mass segregation in this meteoroid

Table 2. Trajectory and radiant data for the double-station GUM meteors imaged in 2010 and 2011 by the Finnish Meteor Network and the Spanish Meteor Network (J2000).

Code	M_v	H_b (km)	H_{max} (km)	H_e (km)	α_g (°)	δ_g (°)	V_∞ (km s^{-1})	V_g (km s^{-1})	V_h (km s^{-1})
FN200110	-3.0 ± 0.5	97.4	–	80.1	230.4	67.1	31.6	29.6	38.6
FN210110	-3.5 ± 0.5	100.0	–	71.0	230.2	66.5	31.9	29.8	38.6
SPMN200110A	1.0 ± 0.5	96.4	–	87.4	229.5	67.5	31.7	29.6	38.6
SPMN200110B	0.0 ± 0.5	94.6	–	84.1	231.0	66.8	31.6	29.5	38.6
SPMN120111A	-2.5 ± 0.5	101.1	–	86.3	225.0	70.3	31.5	29.3	38.4
SPMN120111B	-1.5 ± 0.5	99.5	–	89.0	230.1	69.2	31.6	29.4	38.6
SPMN200111	-5.0 ± 0.5	102.6	72.7	67.3	227.7	67.5	31.7	29.6	38.6

Figure 1. Composite image of the FN200110 GUM meteor, imaged on 2010 January 20 at $17^{h}\,17^{m}\,57 \pm 2$s UTC from Pieksämäki (Finland).

stream because the smaller particles are missing among the members crossing Earth's orbit. The brightest multi-station meteors registered during this observing campaign were imaged from Finland. The first of them (Fig. 1), with a magnitude of -3.0 ± 0.5, was simultaneously recorded from stations 9, 11 and 12 in Table 1 on January 20, at $17^{h}\,17^{m}\,57^{s} \pm 2^{s}$ UTC (code FN200110). The second of these meteors, which is shown in Fig. 2 and had a magnitude of -3.5 ± 0.5, was imaged on January 21, at $21^{h}\,46^{m}\,21^{s} \pm 2^{s}$ UTC, from stations 10 and 12 (code FN210110). From Spain, two additional double-station trails with magnitudes $+1.0 \pm 0.5$ and 0.0 ± 0.5, respectively, were recorded on 2010 January 20 from stations 1 and 3.

During the 2011 observing campaign, the brightest recorded event was the mag. -5.0 ± 0.5 fireball (code SPMN200111) shown in Fig. 3, which was simultaneously imaged from stations 1 and 2 in Spain. But previously, on January 12, two more double-station members of this shower (codes SPMN120111A and SPMN120111B) were imaged from stations 1 and 3, at $3^{h}\,55^{m}\,09\overset{s}{.}4 \pm 0\overset{s}{.}1$ UTC and $23^{h}\,16^{m}\,05\overset{s}{.}7 \pm 0\overset{s}{.}1$ UTC, respectively. During this campaign, five more meteors were observed emanating from this radiant by several SPMN video stations from January 10 to 22, but unfortunately they were not recorded from double stations due to bad weather, and so, no orbits could be derived from them. These trails reveal, however, that 2011 GUM meteors also were relatively bright, with an average visual magnitude of 0.0 ± 0.5 (See Table 3).

For multi-station events, Table 2 contains the calculated values of the beginning and terminal heights (H_b and H_e), the pre-atmospheric, geocentric and heliocentric velocities (V_∞, V_g and V_h), the position (J2000.0) of the geocentric radiant (α_g and δ_g) and the visual magnitude (M_v). Meteor magnitudes have been estimated by performing a direct comparison of the brightness level of the pixels near the maximum luminosity of the meteor trail and nearby stars. On the other hand, the averaged observed pre-atmospheric velocity calculated from the velocities measured at the beginning of the meteor trail was $V_\infty = 31.6 \pm 0.3$ km s^{-1}.

For events listed in Table 2, the convergence angle Q is greater than 20°. This is the angle between the two planes delimited by the observing sites and the meteor path in the triangulation. From the radiant position, appearance time and velocities we derived the orbital elements shown in Table 4 (J2000.0) by following the above-mentioned procedure. These orbits were obtained with our AMALTHEA software and have been compared to the orbital parameters calculated with the METOBS software (Langbroek 2004), and both results coincided.

4 DISCUSSION

4.1 Orbital elements

Table 4 also includes the mean orbital data calculated by taking into account a total of $N = 7$ orbits. With these, a value of Tisserand's

Figure 2. Composite image of the FN200110 GUM meteor, imaged on 2010 January 21 at $21^{\rm h}\,46^{\rm m}\,21 \pm 2$s UTC from Joutsa (Finland).

parameter with respect to Jupiter $T_{\rm J} = 2.55$ is obtained. This suggests that GUM meteoroids are associated with a Jupiter family comet.

On the other hand, the orbital data obtained for the GUM can reveal if these meteoroids are trapped in an orbital resonance with Jupiter. Thus, as the orbital period is proportional to $a^{3/2}$, by taking into account the values of the semimajor axis in Table 4 we can infer the orbital period of the meteoroids. The results are also shown in Table 4. The semimajor axis depends strongly on the observed value of V_∞, and so, the uncertainty in the determination of the velocity gives rise to significant errors in the orbital period. So, a larger number of orbits would be desirable in order to get better results. Despite this, the results reveal that these meteoroids are trapped, within the observational uncertainty, in a 5:2 resonance with Jupiter. The evolution with time of the orbit of this stream was analysed during a time period of 20 000 yr with the MERCURY6 software (Chambers 1999), a hybrid symplectic integrator widely used in Solar system dynamics studies. This analysis revealed that this resonance, which is located at a heliocentric distance of about 2.82 au, is stable. As consequence of such a dynamic mechanism, it is possible that the trapping is biased for moderately large meteoroids. So, this could explain the absence of faint meteors in the displays of this shower. Note that the mean inclination is 44°.8, so these meteoroids have probably been in such stable orbits for centuries (the exact time is unknown). Consequently, this stream could have suffered a similar collisionally erosive process with zodiacal dust as experienced by 51P/Tempel-Tuttle meteoroids (Trigo-Rodríguez et al. 2005).

4.2 Tensile strength

Only the SPMN200111 fireball exhibited flares along its trajectory. These took place at 82.9 and 72.7 km above the ground level, when the velocity was, respectively, of about 29.1 and 26.5 km s^{-1}. These events are typically produced by the fragmentation of the meteoroids when these particles penetrate denser atmospheric regions. Once the overloading pressure becomes larger than the particle strength, the particle breaks apart. Quickly after that, a bright flare is produced as a consequence of the fast ablation of tiny fragments delivered to the thermal wave in the fireball's bow shock. Nevertheless, as can be seen in Fig. 3(a), the first fragmentation experienced by this fireball was not catastrophic, and the remaining material continued penetrating in the atmosphere. The second flare, however, corresponded to a catastrophic disruption of the meteoroid by the end of the fireball's luminous trajectory, and then can be used as a proxy for an estimation of the strength of the particle. The so-called tensile

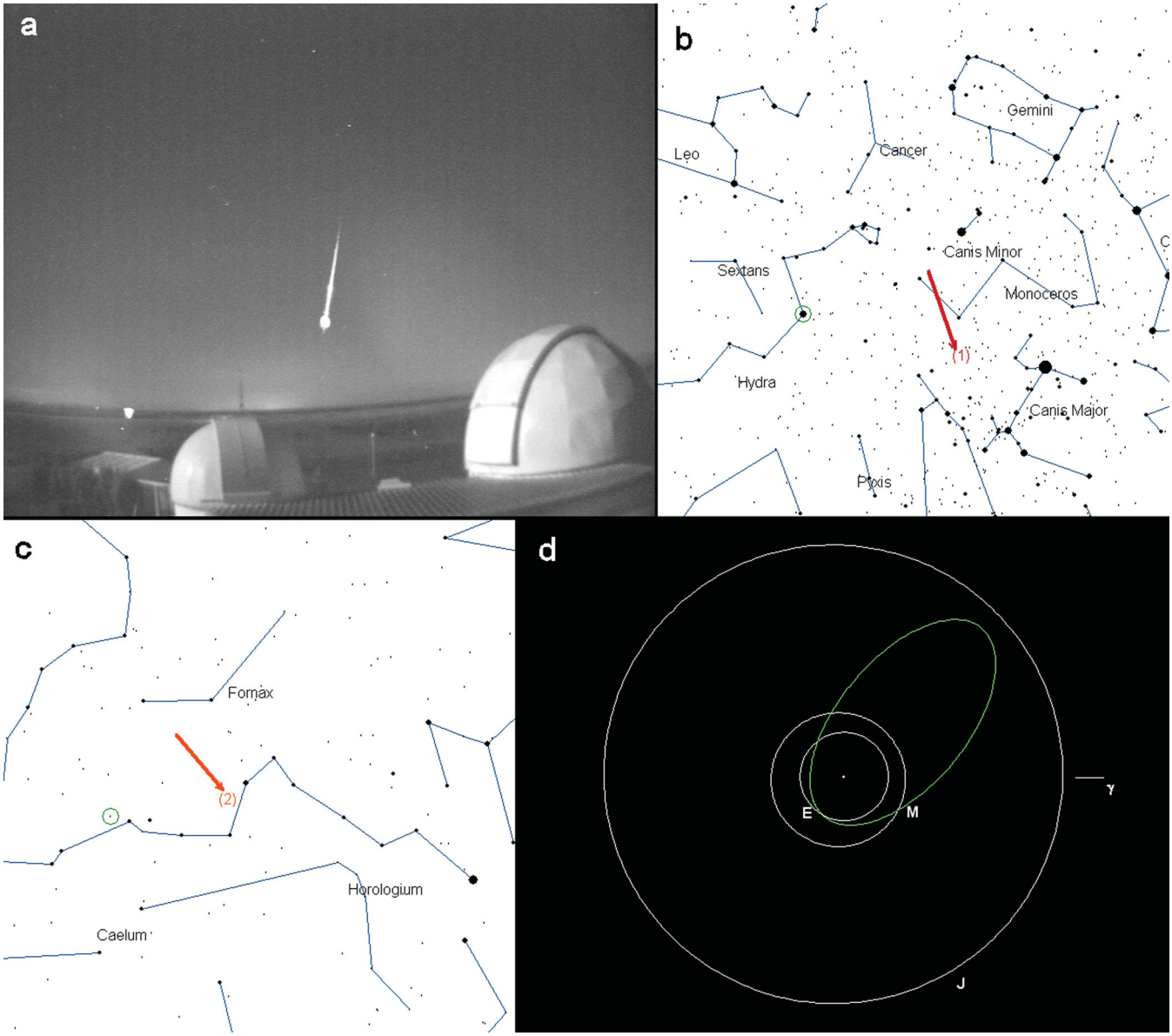

Figure 3. (a) Composite image of the mag. −5.0 ± 0.5 GUM fireball (code SPMN200111) imaged on 2011 January 20 at $20^{h}\ 40^{m}\ 03\overset{s}{.}2 \pm 0\overset{s}{.}1$ UTC over the domes of La Hita Astronomical Observatory (Spain). (b) Apparent trajectory of the bolide as seen from Sevilla and (c) La Hita meteor observing stations. (d) Heliocentric orbit of the meteoroid projected on the ecliptic plane.

(aerodynamic) strength S at which these breakups take place can be calculated from the equation (Bronshten 1981)

$$S = \rho_{\rm atm} v^2, \tag{1}$$

where v is the velocity of the meteoroid at the disruption point and $\rho_{\rm atm}$ the atmospheric density at the height where this fracture takes place. The atmospheric density was calculated from the US standard atmosphere model (U.S. Standard Atmosphere 1976). In this way, we infer that the meteoroid exhibited the first flare under a dynamic pressure of 8.21×10^3 dyn cm^{-2}, while the bright ending flare took place under an aerodynamic pressure of about 3.42×10^4 dyn cm^{-2}. This high value is similar to those found for particles belonging to old streams, such as the Taurids (3.4×10^4 dyn cm^{-2}) and the Quadrantids ($\sim 2\times\ 10^4$ dyn cm^{-2}) (Trigo-Rodríguez & Llorca 2006a, 2007).

4.3 Emission spectrum

Just one of the imaged GUM meteors was bright enough to produce an emission spectrum that could be recorded by one of our CCD video devices equipped with a 1000 lines mm^{-1} transmission grating for meteor spectroscopy. This event was the mag. −5.0 ± 0.5 bolide simultaneously recorded on 2011 January 20 at $20^{h}\ 40^{m}\ 03\overset{s}{.}2 \pm 0\overset{s}{.}1$ UTC (code SPMN200111) from La Hita Astronomical Observatory and Sevilla (Fig. 3). The spectrum, which was imaged from La Hita, was produced during the brightest flare exhibited by this fireball. As this flare corresponds to just one frame in the video file, the evolution with time of this spectrum and the relative loss of sodium versus magnesium as a function of altitude could not be analysed. Such measurements are usually used to provide clues on thermal effects during space weathering exposure (Trigo-Rodríguez, Llorca & Fabregat 2004a; Trigo-Rodríguez & Llorca 2006b). In any case, this spectrum despite of having low

Table 3. Magnitudes of the GUM meteors imaged in 2011.

Magnitude	−6	−5	−4	−3	−2	−1	0	1	2	Total
Number	0	1	0	0	1	1	0	2	3	8

resolution (about 1.2 nm pixel^{-1}) provides an insight into the nature of the meteoroid. It was processed with our CHIMET software (Madiedo, Trigo-Rodríguez & Lyytinen 2011b), which employs the same reduction procedure described in Trigo-Rodríguez et al. (2003). Thus, the video frames containing the emission spectrum were dark frame subtracted and flat-fielded. Then, the spectrum was calibrated in wavelength by identifying typical lines appearing in meteor spectra, such as Ca, Fe, Mg and Na multiplets. The signal was finally corrected by using the spectral sensitivity curve of the recording device. Figs 4(a) and (b) show, respectively, the raw and processed spectrum.

The most noticeable emission lines can be seen in Fig. 4(c). These correspond to Ca I-1 (422.7 nm), Fe I-41 (440.4 nm), Mg I-2 (517.3 nm) and Na I-1 (588.9 nm). The K and H lines of ionized calcium (Ca II), at 393.3 and 396.8 nm, respectively, are also very prominent, although they appear blended because of the low resolution of the spectrum.

To obtain the relative chemical abundances, the procedure was to use a software to reconstruct a synthetic spectrum to be compared with the observed one. We determined four key parameters: temperature (T), the column density of atoms (N), the damping constant (Γ) and the surface area (P) from the observed brightness of lines. The least-squares method is implemented to get the best fit among synthetic and observed spectra. As most lines in the fireball spectrum are of neutral iron, Fe I was taken as a reference element to adjust the intensity of lines and temperature (T). Once T was estimated, the software was allowed to change the column density (N) of any element in order to fit the intensity of lines. Obviously, to obtain the chemical composition, the degree of ionization of different elements must be considered taking into account the ratio of neutral, singly and doubly ionized atoms given by the Saha equation. We remark that the high-temperature component (usually characterized by bright Ca II and Si II lines) was almost non-existent as we expect for low-velocity meteors like the GUM. We also remark that the hot component typically forms less than ∼1 per cent of the meteor vapour envelope in meteors of GUM velocity (see for more details, Borovièka 1994). Consequently, a direct determination of the Si/Fe ratio was not possible from the hot component neither from the main component (both too weak for being clearly identified in our SPMN200111 low-resolution spectrum). A more detailed explanation of the determination of chemical abundances is given in Trigo-Rodríguez et al. (2003), and the full procedure and the related theory were described carefully in Borovièka (1993). The resulting values for the averaged temperature and Fe I column density were 4600 ± 200 K and 10^{18} m^{-2}, respectively. Once these values are fixed, and the Fe I lines were matched in relative intensity, we modified the abundances of the other elements identified in the spectrum in order to get an optimal fit. The calculated abundance ratios referred to Fe are given in Table 5. We notice that the SPMN200111 meteoroid has abundance ratios similar to chondritic, but was depleted in Mg, Ca and Na. This is not so surprising if we take into account that the analysed spectrum was produced during the ending flare, when the particle suffered the last stages of ablation. In fact, differential ablation of Na and Mg along the luminous path of video meteors with similar geocentric velocity has been observed (see e.g. fig. 7 in Koten et al. 2006). Consequently, the bulk chemical ratios inferred from SPMN200111 should be taken with caution, but they encourage us to obtain more detailed and complete GUM emission spectra in the future.

4.4 Parent body

The orbital data obtained in this work can be used to infer information about the likely parent body for the GUM. For this purpose, we have used our ORbital Association Software (ORAS) program, which can search through the Near Earth Objects Dynamic Site (NeoDys) and Minor Planet Center data bases in order to establish a potential link with other bodies in the Solar system (Chesley & Milani 1999). This association between meteoroid streams and other objects in the Solar system is usually done by means of the so-called dissimilarity criteria. These employ a function (the so-called dissimilarity function) to measure the distance between different orbits. The first of these criteria, which was proposed by Southworth and Hawkins, is known as the D-criterion and is based on the values of the semimajor axis, eccentricity and inclination only (Southworth & Hawkins 1963). The improved version of the Southworth and Hawkings criterion, the $D_{\rm SH}$-criterion, also takes into account the longitude of the ascending node and the argument of perihelion. Alternative versions of this criterion have also been developed, including those proposed by Drummon (1981), Jopek (1993), Valsecchi, Jopek & Froeschlé (1999) and Jenniskens (2008). According to this idea, a parent body would be associated with a given meteoroid stream if the dissimilarity function remains below an appropriate cut-off value. In the case of the Southworth and Hawkings criterion, usually $D_{\rm SH} < 0.15$ is adopted in order to validate an association (Linblad 1971a,b). Then, once a candidate is found, a numerical integration backwards in time of the orbital parameters of the potential parent body and the meteoroid swarm should be performed in order to test

Table 4. Orbital elements (J2000) and orbital period for the double-station GUM meteors imaged in 2010 and 2011 by the Finnish Meteor Network and the Spanish Meteor Network. The mean orbit (for $N = 7$ meteors) together with the standard error of the average is included.

Code	a (au)	e	i (°)	Ω (°)	ω (°)	q (au)	P (yr)
FN200110	2.84 ± 0.30	0.664 ± 0.033	48.44 ± 0.61	300.404 ± 10^{-3}	202.16 ± 0.67	0.955 ± 0.005	4.78
FN210110	2.82 ± 0.31	0.661 ± 0.029	48.83 ± 0.41	301.612 ± 10^{-3}	202.40 ± 0.37	0.955 ± 0.005	4.72
SPMN200110A	3.01 ± 0.38	0.671 ± 0.040	48.90 ± 0.57	300.6996 ± 10^{-4}	203.15 ± 0.72	0.957 ± 0.005	5.22
SPMN200110B	2.89 ± 0.32	0.669 ± 0.036	48.54 ± 0.72	300.8787 ± 10^{-4}	202.67 ± 0.57	0.961 ± 0.005	4.91
SPMN120111A	2.78 ± 0.32	0.667 ± 0.021	47.81 ± 0.62	291.4330 ± 10^{-4}	205.31 ± 0.82	0.945 ± 0.005	4.66
SPMN120111B	2.84 ± 0.37	0.668 ± 0.027	48.23 ± 0.67	292.2544 ± 10^{-4}	201.65 ± 0.47	0.955 ± 0.005	4.78
SPMN200111	2.86 ± 0.30	0.661 ± 0.032	48.30 ± 0.51	300.2904 ± 10^{-4}	204.19 ± 0.31	0.949 ± 0.005	4.83
Average ($N = 7$)	2.86 ± 0.31	0.666 ± 0.031	48.44 ± 0.59	298.224 ± 10^{-3}	203.07 ± 0.58	0.954 ± 0.005	4.84

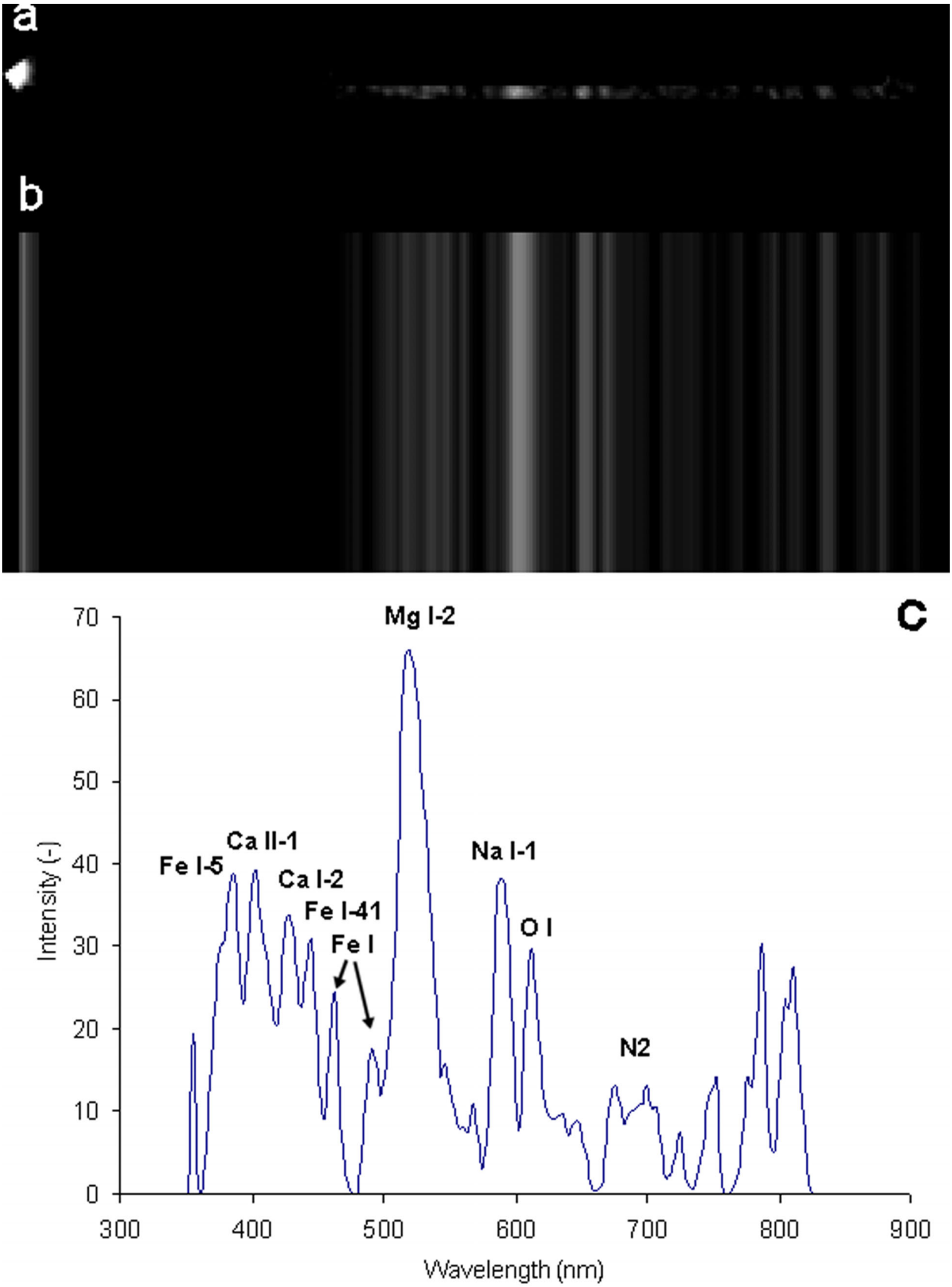

Figure 4. Emission spectrum of the SPMN200111 bolide: (a) raw signal, with the fireball (order zero) on the left; (b) calibrated spectrum; (c) main lines identified in the spectrum, together with their multiplet number (intensity is expressed in arbitrary units).

Table 5. The abundances inferred for the SPMN200111 meteoroid compared with the averaged CI and CM groups of carbonaceous chondrites. We assumed a chondritic ratio Si/Fe = 1.16 to make the conversion of abundances relative to Fe instead of Si (Rietmeijer 2000, 2002a,b; Trigo-Rodríguez et al. 2003).

	Mg/Fe	Ca/Fe	Na/Fe	Mn/Fe	Ni/Fe
SPMN200111	1.0 ± 0.1	0.04 ± 0.01	0.03 ± 0.01	$(8 \pm 1) \times 10^{-3}$	0.08 ± 0.01
CI chondrites	1.23	0.08	0.07	0.01	0.06
CM chondrites	1.20	0.08	0.04	7×10^{-3}	0.05

if the link is just casual or real (Williams & Wu 1993; Williams et al. 2004). This can be done, for instance, by means of the Mercury 6 software (Chambers 1999). However, when this procedure is applied to the average orbit obtained for the GUM, the lowest values obtained for the D_{SH} parameter are of about 0.40. So, the conclusion is that either the parent body of this swarm is not yet catalogued or it was disappeared long time ago. In favour of the last option, dynamic trapping of GUM meteoroids could have preserved this stream longer than the own lifetime of their parent comet. In fact, resonances are known to play an important role in the creation of orphan meteoroid streams (Vaubaillon, Lamy & Jorda 2006).

5 CONCLUSIONS

Despite unfavourable weather conditions, we have characterized the activity of the recently discovered GUM meteor shower during its outburst in 2010 January, but also during 2011 January. Our main conclusions are as follows.

(1) The orbital data obtained from seven multi-station meteors reveal that these meteoroids are trapped in a 5:2 resonance with Jupiter. Besides, the value of Tisserand's parameter indicates that the GUM Minorids are produced by a Jupiter family comet.

(2) The tensile strength of these meteoroids has been estimated and is consistent with fluffy particles of cometary origin.

(3) We have also obtained and analysed an emission spectrum produced by a mag. −5 GUM fireball. The inferred relative abundances of the main elements in the meteoroid support a chondritic nature for the particles in this swarm.

(4) By employing different dissimilarity criteria, our orbital data association software indicates that the parent body of this meteoroid stream is not yet catalogued or it has disappeared.

ACKNOWLEDGEMENTS

We acknowledge Timo Kantola, Mika Järvinen, Ari Jokinen and Ilkka Yrjölä for the images recorded from Finland during the 2010 GUM outburst. Besides, we thank Fundación AstroHita for its support in the establishment and operation of the automated meteor observing station located at La Hita Astronomical Observatory (La Puebla de Almoradiel, Toledo, Spain). We also acknowledge support from the Spanish Ministry of Science and Innovation (projects AYA2009-13227, AYA2009-14000-C03-01, AYA2011-26522 and AYA2011-30106-C02-01), CSIC (grant #201050I043) and Junta de Andalucía (project P09-FQM-4555).

REFERENCES

Borovièka J., 1993, A&A, 279, 627
Borovièka J., 1994, Planet. Space Sci., 42, 145
Bronshten V. A., 1981, Geophysics and Astrophysics Monographs. Reidel, Dordrecht
Brown P., Wong D. K., Weryk R. J., Wiegert P., 2010, Icarus, 207, 66
Ceplecha Z., 1987, Bull. Astron. Inst. Czech., 38, 222
Chambers J. E., 1999, MNRAS, 304, 793
Chesley S. R., Milani A., 1999, BAAS, 31, 1117
Drummond J. D., 1981, Icarus, 45, 545
Jenniskens P., 2008, Icarus, 194, 13
Jenniskens P., 2010, Cent. Bur. Electron. Telegrams, 2146, 1
Jopek T. J., 1993, Icarus, 106, 603
Koten P., Borovička J., Spurný P., Evans S., Štork R., Elliott A., 2006, MNRAS, 366, 1367
Langbroek M., 2004, WGN, JIMO, 32, 109
Lindblad B. A., 1971a, Smiths. Contr. Astrophys., 12, 1
Lindblad B. A., 1971b, Smiths. Contr. Astrophys., 12, 4
Madiedo J. M., Trigo-Rodríguez J. M., 2007, Earth Moon Planets, 102, 133
Madiedo J. M., Ortiz J. L., Castro-Tirado A., Díaz M. J., Trigo-Rodríguez J. M., 2010, 41st Lunar and Planetary Sci. Conf., Houston, Texas, p. 1504
Madiedo J. M., Trigo-Rodríguez J M., Ortiz J. L., Morales N., 2010, Adv. Astron., 2010, 1
Madiedo J. M., Trigo-Rodríguez J. M., Lyytinen E., 2011a, in Cooke W. J., Moser D. E., Hardin B. F., Janches D., eds, Proc. Meteoroids: The Smallest Solar System Bodies, NASA/CP-2011-216469, p. 330
Madiedo J. M., Toscano F. M., Trigo-Rodríguez J. M., 2011b, EPSC-DPS Joint Meeting Vol. 6, Software tools for the analysis of video meteors emission spectra, Nantes, France, p. 72
Rietmeijer F., 2000, Meteorit. Planet. Sci., 35, 1025
Rietmeijer F., 2002a, Chemie der Erde, 62, 1
Rietmeijer F., 2002b, Earth Moon Planets, 88, 35
Southworth R. B., Hawkins G. S., 1963, Smithsonian Contrib. Astrophys., 7, 261
Trigo-Rodríguez J. M., Llorca J., 2006a, MNRAS, 372, 655
Trigo-Rodríguez J. M., Llorca J., 2006b, Adv. Space Res., 39, 517
Trigo-Rodríguez J. M., Llorca J., 2007, MNRAS, 375, 415
Trigo-Rodríguez J. M., Llorca J., Borovicka J., Fabregat J., 2003, Meteorit. Planet. Sci., 38, 1283
Trigo-Rodríguez J. M., Llorca J., Fabregat J., 2004a, MNRAS, 348, 802
Trigo-Rodríguez J. M., Llorca J., Lyytinen E., Ortiz J. L., Sánchez Caso A., Pineda C., Torrell S., 2004b, Icarus, 171, 219
Trigo-Rodríguez J. M., Betlem H., Lyytinen E., 2005, ApJ, 621, 1146
Trigo-Rodríguez J. M., Madiedo J. M., Llorca J., Gural P. S., Pujols P., Tezel T., 2007, MNRAS, 380, 126
Trigo-Rodríguez J. M., Madiedo J. M., Williams I. P., 2009, MNRAS, 394, 569
U. S. Standard Atmosphere, 1976, NOAA-NASA-USAF, Washington
Valsecchi G., Jopek T., Froeschlé C., 1999, MNRAS, 304, 743
Vaubaillon J., Lamy P., Jorda L., 2006, MNRAS, 370, 1841
Williams I. P., Wu Z. D., 1993, MNRAS, 262, 231
Williams I. P., Ryabova G. O., Baturin A. P., Chernitsov A. M., 2004, MNRAS, 355, 1171

This paper has been typeset from a Microsoft Word file prepared by the author.